Analyst

ROYAL SOCIETY OF CHEMISTRY

PAPER

View Article Online
View Journal | View Issue

Cite this: *Analyst*, 2021, **146**, 5102

An integrated microfluidic detection system for the automated and rapid diagnosis of high-risk human papillomavirus†

Xiaoyu Zhao,‡[a] Xiang Li,‡[a] Weihao Yang,[a] Jiwei Peng,[a] Jiajun Huang *[a,b] and Shengli Mi *[a]

Human papillomavirus (HPV) causes the prevalent sexually transmitted infection that accounts for the majority of cervical cancer incidences. Therefore, the development of a rapid, accurate, automatic and affordable nucleic acid detection strategy is urgently required for HPV tests, among which microfluidic chip is a promising diagnostic method. In this work, we developed a microfluidic detection system consisting of a microfluidic chip and the corresponding detection equipment to diagnose high-risk HPV. The proposed method integrates nucleic acid purification, isothermal amplification and real-time fluorescence detection into one device. Moreover, it demonstrates good detection performance such as high specificity of primer sets (100%) and exceptional stability (coefficient of variation <6%) among five HPV genotypes. Besides, the microfluidic loop–mediated isothermal amplification (LAMP) assay is accurate (specificity of 91.7% and sensitivity of 100%) and fast (average time threshold = 10.56 minutes) when considering the conventional qPCR assay as the gold standard. The integrated microfluidic detection system offers automated and rapid diagnosis within 40 minutes and shows broad potential to deliver point-of-care detection in resource-limited circumstances owing to its simplicity and affordability.

Received 12th April 2021,
Accepted 27th June 2021

DOI: 10.1039/d1an00623a

rsc.li/analyst

Introduction

Human papillomavirus (HPV) causes the most common sexually transmitted infection worldwide and has become a well-established oncogenic viral factor in cervical cancer as well as other anogenital cancers.[1] Moreover, the prevalence of high-risk HPV infection typically correlates with cervical cancer development; meanwhile, the correlation steadily enhances with age.[2] The burden of cervical cancer and other HPV-related cancers is rising drastically, and approximately over 100 000 new cervical cancer cases are diagnosed annually in China, according to the HPV Information Centre.[3] Therefore, diagnostic screening programs, particularly for high-risk clades, are responsible for a substantial decline in cervical cancer incidence and mortality.[4] Conventional screening for cervical cancer is cytological testing, in which patients suffer, and hence, this method relies on skillful physicians.[5] Hence, molecular detection of HPV has become the gold standard to identify the virus and determine its specific type.[6] However, the current DNA diagnosis methods of HPV such as Qiagen HPV Sign Genotyping Test,[7] Roche cobas® HPV Test[8] and Hologic Aptima HPV Assay[9] require sophisticated instruments and elaborate processes, which are time-consuming and uneconomic. Therefore, fast, accurate, cost-effective and high-throughput approaches are urgently required for the detection of HPV, among which microfluidic detection technology has emerged as an attractive point-of-care diagnostic tool.

The microfluidic chip allows precise manipulation on a small amount of fluids and has been developed rapidly since its excellent potential to conduct multiple complicated assays on a chip, the so-called "lab-on-a-chip".[10] The centrifugal microfluidic chip is evidently one of the most prevalent microfluidic platforms.[11] It integrates various operations such as liquid motivation, distribution and retention into a single chip with the aid of centrifugal force, unlike other microfluidic chips, which require external syringe pumps, tubes and complex accessories.[12] In particular, the centrifugal microfluidic system could achieve automatic and high-throughput experiments with vastly reduced reagents and costs.[13] Therefore, the centrifugal microfluidic chip has drawn wide-

[a]*Bio-manufacturing Engineering Laboratory, Tsinghua Shenzhen International Graduate School, Tsinghua University, Shenzhen, China*
[b]*Optometry Advanced Medical Equipment R&D Centre, Research Institute of Tsinghua University in Shenzhen, Nanshan District, Shenzhen, China*

†Electronic supplementary information (ESI) available. See DOI: 10.1039/d1an00623a

‡These authors contributed equally to this work.

spread attention and showed tremendous promise in the field of cell culture,[14,15] chemical analysis,[16,17] drug screening,[18,19] and especially molecular diagnostics.[20–22] In addition, it has been developed into timely and simple nucleic acid detection devices, which could detect pathogens early, prevent disease transmission and reduce mortality. There are several microfluidic platforms established for nucleic acid detection of the African swine fever,[23] human respiratory coronaviruses,[24] and foodborne pathogen,[25] which provide huge accessibility to point-of-care test. However, most microfluidic devices generally exclude the nucleic acid extraction process from the nucleic acid assay since sample preparation is complicated and time-consuming.[24,26] In addition, a few studies integrate traditional nucleic acid extraction methods into the detection system, yet inevitably complicating the device and introducing amplification inhibitors.[27–29] Therefore, a simple, rapid, cost-effective and all-in-one microfluidic detection system remains to be constructed.

Conventionally, the molecular diagnostics method based on nucleic acid is dominated by the variable temperature amplification, represented by polymerase chain reaction (PCR) typically.[30] The PCR assay is the most common method for nucleic acid amplification and detection, owing to its excellent accuracy. However, it demands precise temperature cycling, sophisticated instruments and relatively long amplification time, which is not suitable for point-of-care testing (POCT). As a result, the novel isothermal amplification methods represented by loop-mediated isothermal amplification (LAMP),[31] recombinase polymerase amplification (RPA)[32] and strand displacement amplification (SDA)[33] have been developed rapidly. Among these, LAMP exhibits outstanding features involving good accuracy, reduced amplification time, high tolerance to impurities and therefore stable reaction conditions. More interestingly, LAMP is compatible with microfluidic chip technology due to its simplicity and constant amplification temperature. Therefore, it has been considered a favorable method to be applied in microfluidic detection.[34]

Here, we established an integrated microfluidic detection system comprising a microfluidic chip, a centrifugal platform, a temperature control plate and a fluorescence detector, which achieved automatic and rapid diagnosis of five high-risk clade HPV types. The proposed method realized three core functions for POCT: nucleic acid purification, isothermal amplification and real-time fluorescence detection. We designed a centrifugal microfluidic chip with easy manufacturing and low cost, in which the whole detection operation was automatically controlled by the default rotation program. We occupied Chelex-100 resin particles to adsorb impurities and amplification inhibitors and separate them through centrifugal motivation and size exclusion, which is a simple and efficient method to purify nucleic acid. The system displayed promising detection performance in terms of high specificity of primer sets with no cross-reaction, good stability under diverse conditions and decent semi-quantitative results similar to the qPCR assay. Besides, the whole process from nucleic acid extraction to centrifugal operation to real-time detection was accomplished within 40 minutes, and the system was capable of performing 40 detections simultaneously for high-throughput preliminary selection. Accordingly, the proposed microfluidic detection system could serve as a rapid, cost-effective and accessible diagnostic tool and has the potential to provide an alternative to qPCR assay, particularly in the context of resource-limited circumstance.

Experimental

Reagents and materials

Human umbilical vein endothelial cells (HUVECs) and HeLa cells were obtained from the National Collection of Authenticated Cell Cultures (Shanghai, China). Cell culture reagents including DMEM-Hi glucose medium, penicillin/streptomycin, fetal bovine serum (FBS) and phosphate buffered saline (PBS) were all purchased from Gibco, Thermo Fisher Scientific (Waltham, MA, USA). All aqueous solutions were prepared in sterilized, distilled water (18.2 MΩ cm at 25 °C). Bst 2.0 WarmStart DNA Polymerase, 10× Isothermal Amplification Buffer, deoxynucleotide solution (dNTP Mix) and magnesium sulfate ($MgSO_4$) were purchased from New England Biolabs (Ipswich, MA, USA). EvaGreen Dye dissolved at 20× and Chelex-100 Resin (sodium form, 100–200 mesh particle size) were obtained from Biotium (Hayward, CA, USA) and Sigma-Aldrich (St Louis, MO, USA), respectively. Betaine anhydrous and 1× TE buffer (10 mM Tris-HCl, 0.1 mM EDTA, pH 8.0) were purchased from Sangon Biotech (Shanghai, China). The TIANamp Genomic DNA Kit and Magnetic Universal Genomic DNA Kit were obtained from TIANGEN Biotech (Beijing, China), and the Universal Blue qPCR SYBR Green Master Mix was obtained from Yeasen Biotech (Shanghai, China). Plasmids carrying highly conserved sequences of HPV were purchased from the National Institutes for Food and Drug Control (Beijing, China). Primers were synthesized and purified by Huada Genomics Technology (Beijing, China), and information on their sequences is listed in Tables S1–S3.†

Cell culture

HUVEC and HeLa cell lines were cultured and incubated in a DMEM-Hi glucose medium supplemented with 10% fetal bovine serum and 1% penicillin–streptomycin at 37 °C in a 5% CO_2 in air atmosphere.

Formulation of LAMP assay

A relatively stable formula of LAMP assay for HPV diagnosis was explored and optimised. The final volume of the individual LAMP reaction was reduced from 25 μL to 8 μL, maximising cost savings and adapting to microfluidic detection. It was composed of 20 mM Tris-HCl, 10 mM $(NH_4)_2SO_4$, 50 mM KCL, 8 mM $MgSO_4$, 0.1% Tween® 20, 1.4 mM dNTP Mix, 320–720 U mL^{-1} Bst 2.0 WarmStart DNA polymerase, 1.6 μM FIP/BIP Primers, 0.2 μM F3/B3 Primers, 0.4 μM LoopF/B Primers and

78 μM Betaine. The LAMP reaction was carried out at 65 °C for 30 min directly on the proposed microfluidic chip.

Microfluidic chip and the matched detection equipment

The microfluidic detection chip comprised five sections. Each consisted of a LAMP cocktail reservoir, a sample chamber, a holding chamber, a mix channel, a collection chamber, an aliquoting structure, a waste chamber and eight reaction chambers (Fig. 1a). The LAMP cocktail reservoir and the holding chamber accommodated the LAMP cocktail, containing 10× Isothermal Amplification Buffer, dNTP mix, $MgSO_4$, EvaGreen Dye and Bst 2.0 DNA Polymerase. The sample chamber contained the sample and Chelex-100 resin for nucleic acid isolation. The mix channel mingled the LAMP cocktail and purified nucleic acid while the collection chamber collected the mixture. After the solution is mixed, the aliquoting structure facilitated equal liquids division and distribution into the reaction chambers, where pre-stored dried LAMP primer sets for subsequent *in situ* isothermal amplification and detection. Meanwhile, the waste chamber held excess waste solution without affecting detection.

The digital photograph of the microfluidic detection chip is demonstrated in Fig. 1b. It was made of polymethyl methacrylate and fabricated using computer-numerical control (CNC) machining equipment (Hongyang Lase, Beijing, China) while applying a pressure sensitive adhesive (PSA) foil layer (WK1501, WowKing material, Taizhou, Zhejiang, China) to seal the structure and form the integrated microfluidic chip (Fig. 1c). Detailed information about the dimensions of the microfluidic chip is provided in Fig. S1.†

The matched detection system's construction was composed of a centrifugal platform, a temperature control plate and a fluorescence detector (Fig. 1d and e). The custom-made centrifugal platform incorporated a servo motor (YZ-57BLS120) and a controller (YZ-ACSD608), both from Yizhi Technology (Hangzhou, Zhejiang, China). The centrifugal module provided precise and sequential control of rotation and achieved specific liquid flow. The temperature control module included a silicone heating film (JK-002, Jiukou Electric Heating Equipment, Wuxi, Jiangsu, China) to maintain 65 °C for the LAMP reaction and its temperature-control precision could reach ± 0.5 °C. The fluorescence detector combined a 460–470 nm light-emitting diode ($LED_{460–470\ nm}$, 3 W,

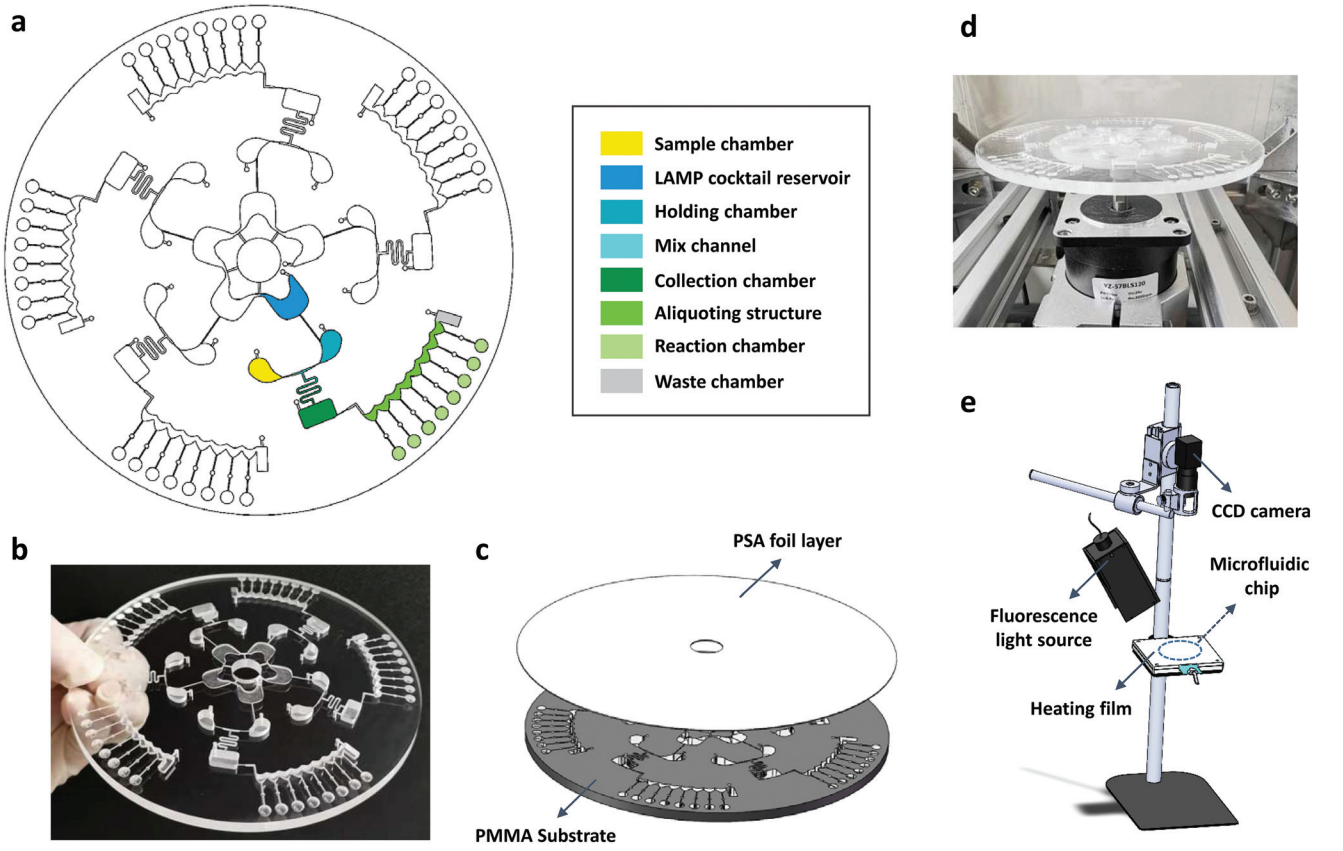

Fig. 1 Schematic of the microfluidic chip and the matched detection equipment. (a) Design of the microfluidic chip, which integrated a sample chamber, a LAMP cocktail reservoir, a holding chamber, a mix channel, a collection chamber, an aliquoting structure, eight reaction chambers and a waste chamber. (b) Digital photograph of the microfluidic chip. (c) Assembly of a CNC-fabricated PMMA substrate and a PSA foil layer to form an integrated microfluidic chip. (d) Digital images of the centrifugal platform. (e) Diagram of the temperature control plate and the fluorescence detector.

Shenzhen Jialetuo Technology, Shenzhen, Guangdong, China), a CCD camera (MS-GED130-T, MTWi Technology, Shenzhen, Guangdong, China) and light filters (YZ-470ZDLGP-X, Yizheng Electronics, Beijing, China; HS-532ZDLGP-Y30, Huangshang Jiguang, Shanghai, China). The $LED_{460–470\ nm}$ illumination served as the light source while EvaGreen Dye emits fluorescence by forming a dye-DNA complex. The CCD camera was used to monitor real-time fluorescence signals. Light filters were assembled into the fluorescence light source and the CCD camera to filter undesired light.

Operation of the microfluidic detection system

The microfluidic detection system integrated nucleic acid purification, isothermal amplification and detection into one chip. The overall schematic depiction of the operation mediated by centrifugal force is shown in Fig. 2. The entire microfluidic isothermal amplification and detection procedures were concluded as below. Various dried primer sets were deposited in the reaction chambers previously. First, the LAMP cocktail and sample were injected into the petaloid reservoir and the sample chamber, respectively (Fig. 2a and b). The LAMP cocktail was evenly distributed into the holding chamber when the microfluidic chip was rotated clockwise. In the meantime, the sample stayed on the spot due to capillary force and Chelex-100 exerted nucleic acid purification (Fig. 2c), where the designed capillary valve realized retention of samples. Then, the microfluidic chip was centrifuged to release the LAMP cocktail and purified nucleic acid, and mix them thoroughly while flowing through the mix channel (Fig. 2d). Afterwards, the mixture reached the collection chamber and was allocated into reaction chambers precisely at two steps of centrifugal forces, in which the aliquoting structure promoted uniform distribution and drove excess solution into the waste chamber (Fig. 2e and f). Table 1 outlines the centrifugal speed control protocol for the operation of the integrated microfluidic detection system. Multiple primer sets were dissolved in the mixture and ultimately formed a homogenous reaction solution. Subsequently, the reaction chamber was heated to 65 °C to activate the LAMP reaction since the chip was in direct contact with the temperature control plate. Following that, real-time fluorescence signals were recorded and monitored using a fluorescence detector. When the LAMP reaction was com-

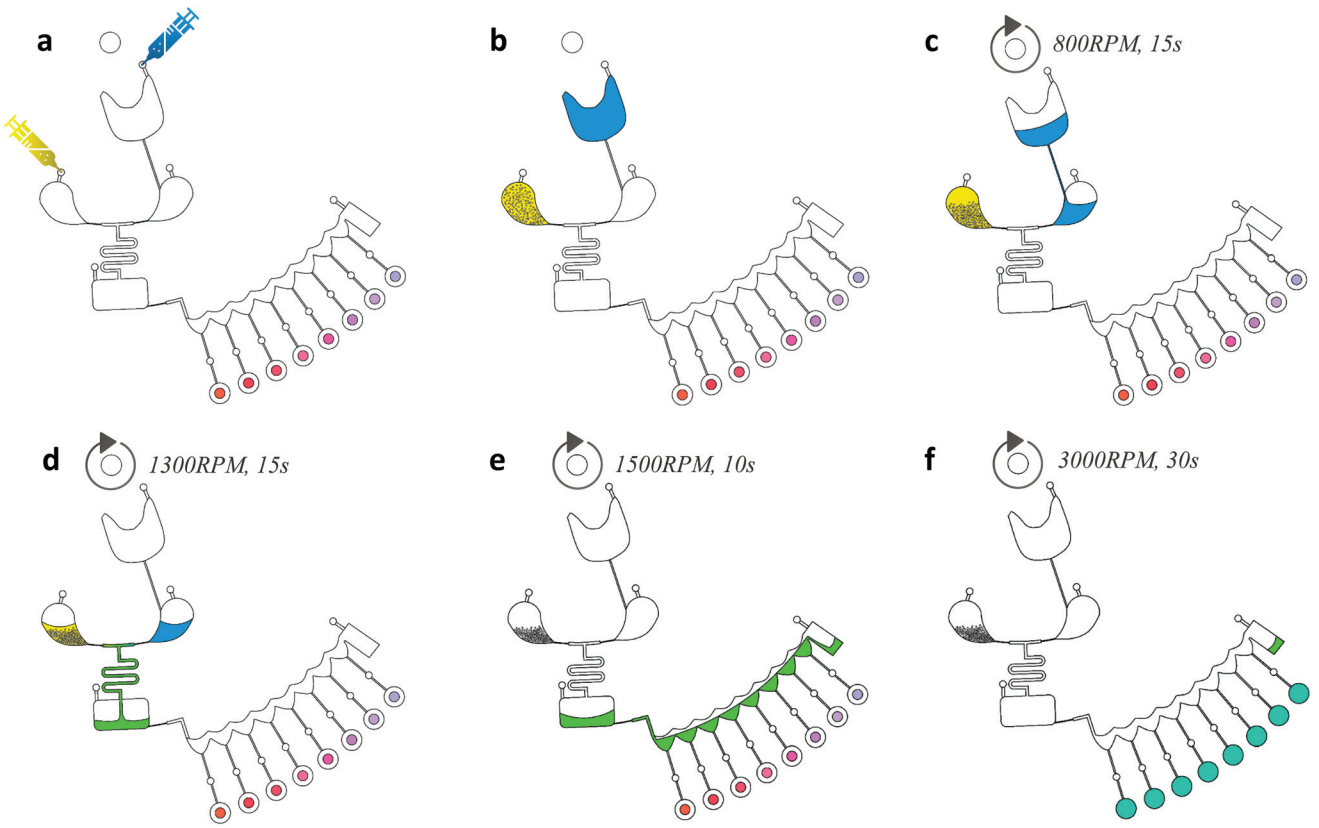

Fig. 2 Overall depiction of the microfluidic chip operation mediated by centrifugal force. (a) LAMP cocktail (blue) and sample (yellow) enter our microfluidic chip *via* injection, whose reaction chambers are embedded with the dried LAMP primer sets (pink and purple). (b) Initial state for subsequent automatic detection. (c) LAMP cocktail flows into the holding chamber. (d) LAMP cocktail blend with purified nucleic acid through the mix channel while the collection chamber accommodates the mixture (green). (e) LAMP reaction mixture is equally aliquoted and excess solution flows into waste chamber. (f) Amplification solution fills reaction chambers and dissolves the pre-deposited primer sets, resulting in eight uniform LAMP reaction mixtures (blue–green). The isothermal amplification and the real-time fluorescence detection inside reaction chambers occur at 65 °C, simultaneously.

Table 1 Centrifugal speed control protocol for microfluidic chip operation

Step	Acceleration (RPM s^{-1})	Speed (RPM)	Time (s)	Operation
1	3000	800	15	Deliver LAMP cocktail
2	3000	1300	15	Release and mix LAMP cocktail and purified nucleic acid
3	1000	1500	10	Allocate LAMP mixture into aliquoting structure
4	3000	3000	30	Distribute LAMP mixture into reaction chamber
5	−3000	0	NA	End centrifugation and initiate LAMP

pleted, the amplification curve would be generated automatically for further investigation. Moreover, to guarantee the accuracy of the microfluidic detection system, agarose gel electrophoresis was conducted to double confirm amplification products.

Nucleic acid purification and assessment

To assess the microfluidic nucleic acid purification efficiency, we engaged four nucleic acid purification methods and used HUVEC as extraction samples in this study. First, the Chelex-100-based microfluidic nucleic acid purification process is illustrated as follows: Chelex-100 Resin, 20% (W/V), was suspended in 1× TE buffer (pH = 8.0) as the nucleic acid purification reagent, which could adsorb impurities and amplification inhibitors effectively.[35] At the initial state, HUVEC cells lysed at 95 °C along with the purification reagent were simultaneously introduced into the sample chamber. The mixture stayed in the sample chamber for several minutes, which allowed Chelex-100 resin particles to adsorb non-nucleic acid impurities and amplification inhibitors comprehensively. Then, Chelex-100 was blocked in the sample chamber owing to size exclusion through centrifugation easily, and the purified nucleic acid solution would be isolated and used for the following analysis. Secondary, the pyrolysis was conducted at 95 °C to lyse cells without other purification processes, as a comparison to the Chelex-100 method. Besides, we utilized two commercially available DNA extraction kits: TIANamp Genomic DNA Kit (hereafter referred to as commercial kit A) and Magnetic Universal Genomic DNA Kit (commercial kit B), as certified standards to evaluate microfluidic nucleic acid purification performance. The DNA extraction experiments were performed in accordance with the official protocol strictly. The nucleic acid quality was collectively determined in aspects of concentration, A260/280 ratio and A260/230 ratio using a NanoDrop 2000c Spectrophotometer (Thermo Fisher Scientific, Waltham, MA, USA). To characterize the impact of non-nucleic acid impurities on the amplification, we employed qPCR analyses targeting the β-actin gene and investigated cycle threshold (Ct) values, which could provide semi-quantitative references in nucleic acid quality evaluation.

Evaluation of the performance of the microfluidic detection system

The performance of the microfluidic detection system was evaluated from three aspects: specificity of primer sets, stability of LAMP assay and comparison with qPCR assay for HPV diagnosis. Five types of high-risk HPV (HPV16, HPV18, HPV39, HPV45, and HPV52) were studied to evaluate the microfluidic detection system's specificity. The cross-reactivity tests, using HPV plasmids as samples, were conducted following the operation of the microfluidic detection system mentioned before. Five specific HPV-targeted primer sets were lyophilized and preloaded in reaction chambers to perform the microfluidic LAMP reaction and verify specificity. Stability trials engaging five types of high-risk HPV were repeated twelve times for strong positive samples (10^6 copies per μL) and weak positive samples (10^3 copies per μL), intending to validate the stability and reproducibility of the developed microfluidic detection system. Furthermore, HeLa cells were used as samples for the conventional qPCR assay and microfluidic LAMP assay. The sensitivity and specificity were analyzed, the receiver operating characteristic (ROC) curves were plotted, and the amplification time based on these two methods was compared to assess the effectiveness.

Statistical analysis

The collected fluorescence signals and amplification curves were analyzed and generated in Matlab (Version 2020b, The MathWorks, Inc., Natick, MA, USA). The qPCR assay was conducted, and the results were analyzed using the StepOnePlus™ Real-Time PCR System (Applied Biosystems, California, USA). The ROC curve was plotted by MedCalc (MedCalc Software, Ostend, West Flanders, Belgium). Other data visualization and statistical analyses were performed using GraphPad Prism 7 (GraphPad Software, La Jolla, CA, USA). Data are presented as mean ± standard deviation (SD) unless otherwise stated. The statistical significance was determined by Student's *t*-test and analysis of variance (ANOVA), indicating as $*p < 0.05$, $**p < 0.01$, $***p < 0.001$ according to the level of significance.

Results and discussion

Mechanism of the centrifugal microfluidic chip

The manipulation of the developed microfluidic chip was illustrated above. In general, we utilized the centrifugal force to motivate liquid propulsion, employed capillary valves to delay liquid release, and integrated aliquoting structures to facilitate equal liquid distribution. Primarily, pyrolysed cell samples along with Chelex-100 purification suspension and LAMP cocktail were introduced into the microfluidic chip simultaneously. Centrifugal force served as the primary driving force

for liquid mixing and flow in the microfluidic detection system. LAMP cocktail was released from the petaloid reservoir into the holding chamber *via* first rotation; meanwhile, a special designed capillary valve restricted the sample *in situ*. Capillary valves are passive valves operated by surface tension and have become prevalent tools in the microfluidic device.[36] Besides, the capillary breakthrough in the centrifugal microfluidic device correlates with an increase in the rotation speed drastically.[37] To ease the burden of centrifugal equipment and simplify the control program, we adjusted and optimized the included angle between capillary valves and the chip's radical direction, facilitating the liquid flow and leading to a lower speed requirement for passing capillary valves. After that, the chip stayed still for a minute and allowed Chelex-100 resin to adsorb non-nucleic acid impurities and LAMP inhibitors. The second rotation with an elevated speed propelled the LAMP cocktail and purified nucleic acid to move forward, mix soundly through an S-shaped microchannel, and transport into the collection chamber. Through the third rotation, the LAMP mixture was further divided into equal volumes of aliquots with the assistance of aliquoting structure. The surplus solution remained in the waste cavity without affecting subsequent reactions. This aliquoting structure permitted the precise aliquot and meter, which neither required expensive manufacture nor complicated design, therefore, exhibited great potential for liquid automation and parallelization in centrifugal microfluidic devices.[38] Next, LAMP mixtures were centrifuged into reaction chambers at a higher speed and dissolved HPV primer sets, which were lyophilized and embedded in reaction chambers previously. Eventually, the homogenous LAMP reaction solution was prepared for isothermal amplification once the temperature reached 65 °C, and fluorescence signals were detected and analyzed simultaneously in real time. Consequently, we adopted some universal components like an S-shaped mix channel, aliquoting structures, and solution reservoirs, and arranged the structures along the radial direction to maximize the effect of centrifugal force, similar to the previous works.[22,26,28] Furthermore, we optimized capillary valves and connecting microchannels, abandoned other complicated phase-change valves, and designed the chip as easy as possible to facilitate low-cost manufacture. In the experimental stage, chips were fabricated using CNC and sealed with biocompatible PSA. In the future, chips can be processed by injection molding and hot pressing for mass production, leading to a much lower unit price than the soft lithography or mechanical processing.[39] Moreover, the all-in-one microfluidic chips are equipped with compatible apparatuses that provide centrifugal force, temperature control and fluorescence monitoring to accomplish automated and effective nucleic acid purification, amplification and detection.

Microfluidic nucleic acid purification efficiency assessment

Nucleic acid purification is the primary procedure in molecular diagnosis, which significantly determines nucleic acid detection. The rapid advancements and innovations in microfluidic research boost the integration of complicated nucleic acid purification into the microfluidic detection system. Thereby, more approaches to microfluidic nucleic acid purification emerge[40] including magnetic beads with active groups,[41–43] silicon-based solid-phase extraction[27,29,44–46] and paper-based microfluidic chips.[47–49] Besides, alternative methods have been developed for microfluidic nucleic acid extraction, among which Chelex-100 chelating resin is an accessible choice. Chelex-100 could selectively adsorb non-nucleic acid impurities and amplification inhibitors. Therefore, it has been extensively developed as a medium for rapid DNA extraction and PCR in forensic cases.[35,50,51] It is also reported that Chelex-100 has massive potential for combining with a microfluidic system and achieve nucleic acid isolation.[52] Accordingly, we occupied Chelex-100 chelating resin as nucleic acid purification suspension and integrated it into the chip, which perfectly accommodated the centrifugal device and entire analysis procedures. Here, we analysed the unusual compatibility between Chelex-100 and our system in the following aspects. First, the LAMP assay is extremely sensitive and pretty resistant to contamination since its detection limit could reach a few copies.[31] Hence, we considered that Chelex-100-based microfluidic nucleic acid purification was fully qualified to meet the LAMP assay standard. It was also worth noting that the Chelex-100-based purification process only requires few minutes. The operation was straightforward compared to conventional nucleic acid extraction methods including multiple complex procedures such as wash and elution. Additionally, we designed the microchannel dimension slightly smaller than the diameter of Chelex-100 particles, so they could be separated from the purified nucleic acid solution and blocked in the sample chamber owing to size exclusion.

We then evaluated the Chelex-100-based nucleic acid purification performance including nucleic acid concentration and A260/280 along with A260/230 ratios and compared it with pyrolysis and commercial extraction kits. The nucleic acid concentration represents the quantity of nucleic acid acquired, while A260/280 and A260/230 ratios are commonly developed to determine the protein contamination and presence of organic contaminants, respectively.[53] The nucleic acid concentration extracted by Chelex-100, pyrolysis, commercial kit A and commercial kit B was 333.0, 373.0, 164.2 and 108.6 ng μL^{-1}, respectively (Fig. 3a). The A260/280 and A260/230 ratios of Chelex-100 were 1.69 and 0.74, respectively (Fig. 3b). These results indicated that the extraction capability of Chelex-100 *via* direct purification and adsorption was decent since there was no nucleic acid loss caused by liquid transfer or non-specific adsorption. However, the purity of nucleic acid extracted by Chelex-100 was inferior to that obtained from commercial kits, signifying that the removal of non-nucleic acid impurities was incomplete and had an upper limitation. We further performed qPCR analysis and assessed the Ct values to reveal whether nucleic acid purified by Chelex-100 was qualified enough for the amplification. The Ct is a semi-quantitative value suggesting the target nucleic acid concentration broadly, which means that a low Ct represents a high

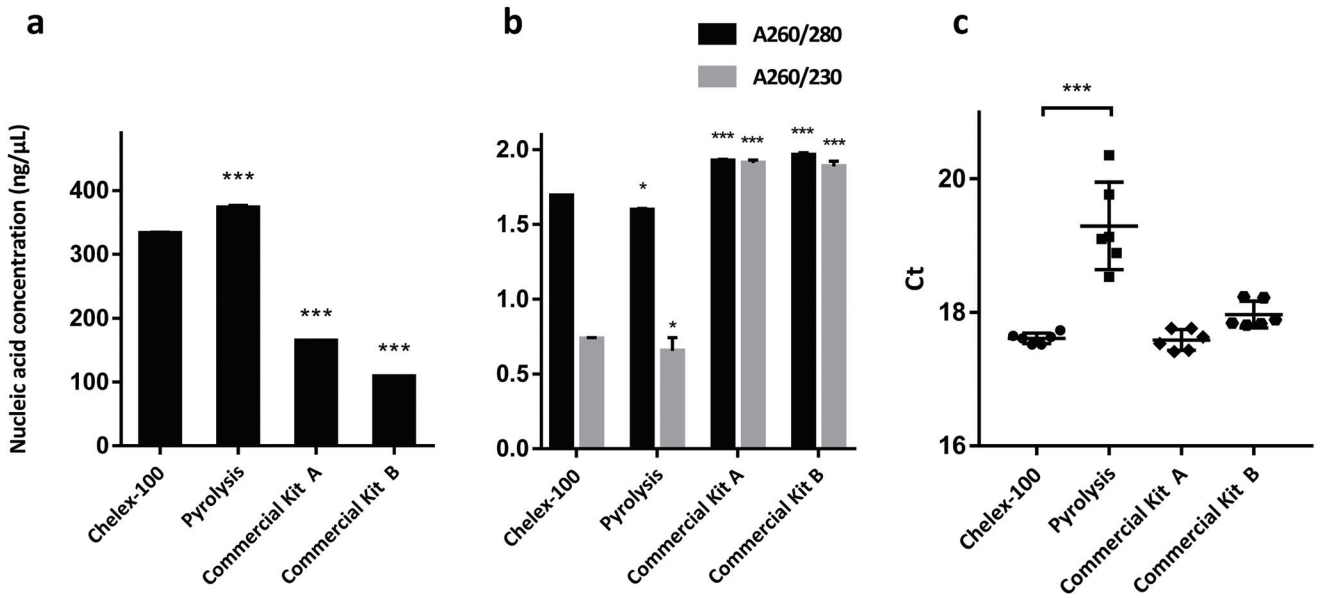

Fig. 3 Assessment of the nucleic acid purification efficiency. (a) Nucleic acid concentration between Chelex-100, pyrolysis, commercial kit A and commercial kit B (n = 3). (b) A260/280 ratio (black) and A260/230 ratio (grey) between Chelex-100, pyrolysis, commercial kit A and commercial kit B (n = 3). (c) Ct value of qPCR assays in which nucleic acid was purified using Chelex-100, pyrolysis, commercial kit A and commercial kit B, respectively (n = 6). Data are presented as mean ± S.D., *p < 0.05, **p < 0.01, ***p < 0.001.

concentration while a high Ct indicates the opposite.[54] The average Ct values of Chelex-100, pyrolysis, commercial kit A and commercial kit B were 17.61, 19.3, 17.59 and 17.97, respectively (Fig. 3c). The Ct value of Chelex-100 was similar to commercial kits and lower than pyrolysis. Moreover, the SD of pyrolysis was 0.6562, which was higher than other groups significantly, indicating the lack of stability. The amplification curves of these four extraction methods are shown in Fig. S2.† These results indicated that Chelex-100 could extract nucleic acid effectively with comparable amplification ability to two commercial kits. Simultaneously, with comparison to the pyrolysis, it was reasonable to confirm that impurities remaining in Chelex-100 purification showed a negligible adverse effect on nucleic acid amplification. Consequently, the nucleic acid isolated by Chelex-100 was competent to carry out isothermal amplification in the microfluidic chip, considering that the concentration of nucleic acid was acceptable and the majority of impurities together with interferences were adsorbed by Chelex-100. As a result, we assured the applicability of Chelex-100 in microfluidic nucleic acid purification and amplification from both theoretical and practical perspectives, and employed it in this detection system. To conclude, we used Chelex-100 particles to adsorb non-nucleic acid impurities and amplification inhibitors instead of traditional complex extraction methods because LAMP is sensitive and has a high tolerance to impurities in samples. The microfluidic chips easily separate particles *via* centrifugal force and size exclusion. This approach is simple, fast (only takes a few minutes), cost-effective and very compatible with our detection system, breaking through the challenge of constructing an integrated microfluidic device.

Diagnostic performance evaluation of the microfluidic detection system

To evaluate the performance of the microfluidic detection system, we used the established microfluidic chip equipped with centrifugal, temperature control and fluorescence detection modules to detect five high-risk HPV, including HPV16, HPV18, HPV39, HPV45 and HPV52. Plasmids carrying highly conserved HPV-L1 genes were applied as positive samples to complete diagnoses following the above workflow. The specificity of primer sets is regarded as an essential factor in nucleic acid detection.[55] Hence, we predominantly explored the specificity of primer sets by multiplex microfluidic LAMP assays. The amplification curves of HPV16, HPV18, HPV39, HPV45, and HPV52 are presented in Fig. 4a–e, respectively. Significant positive sigmoid amplification curves occurred when the samples met the corresponding primer sets; otherwise, the negative flat line took place. Besides, the positive reaction chambers produced intense fluorescence signals, which were at least five times stronger than negative responses (Fig. 4f). These results indicated that the developed microfluidic system exhibited high specificity among five high-risk HPV genotypes in cross-reactive tests, which was a prerequisite in clinical diagnosis.

Stability is a crucial indicator to evaluate the performance of a molecular detection system as well. The proposed microfluidic detection system utilized strong and weak positive samples (10^6 and 10^3 copies per μL) of five genotypes of HPV to conduct duplicated experiments twelve times. We analyzed and investigated the time threshold (Tt) values for each amplification curve as critical criteria and then calculated the SD and coefficient of variation (C.V.) to examine the stability stat-

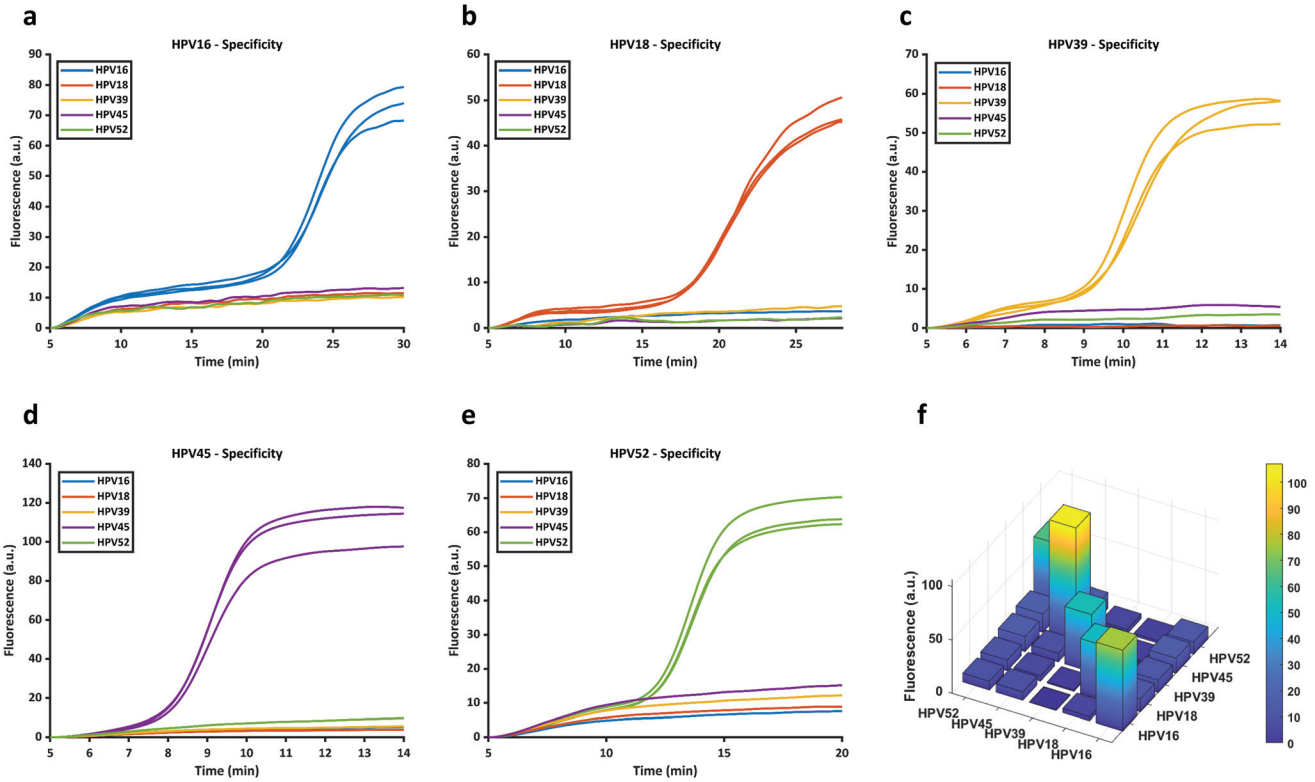

Fig. 4 Evaluation of the specificity of the microfluidic detection system. Cross-reactivity tests for (a) HPV16; (b) HPV18; (c) HPV39; (d) HPV45; and (e) HPV52. (f) Histogram overview of specificity analysis.

istically. The results in Fig. 5a–e manifested the amplification curves and Tt values of strong and weak samples in HPV genotype diagnosis using our system. There were significant differences ($p < 0.001$) in Tt values between strong and weak positive samples, which supported encouraging stability under diverse conditions. Fig. 5f shows the SD and C.V. values following all the assessment of twelve replicate trials of strong and weak positive samples. In addition, exact Tt values of specificity and stability are provided in Tables S4 and S5.† HPV 16, the C.V. values for strong and weak samples were 5.11% and 4.80%, and the C.V. values for strong and weak HPV18 samples were 3.85% and 4.71%, respectively. In HPV39, HPV45, and HPV52, the C.V. values of strong and weak samples ranged from 5.03% to 4.08%, 3.16% to 4.81% and 5.10% to 5.06%, separately. These results indicated high specificity of primer sets and stability of our microfluidic detection system, which guaranteed reliability. Collectively, the microfluidic detection system expressed promising diagnostic performance for the HPV test in terms of specificity and stability, which implied potential application in POCT.

Comparison between conventional qPCR assay and microfluidic LAMP assay

PCR is a revolutionary technology that has been considered as the gold standard for nucleic acid detection currently.[56] HeLa cell is a remarkable human cell line, in which HPV18 DNA is integrated and amplified in its cellular genome.[57] Following that, to further verify the microfluidic detection system's ability, we enrolled HeLa cells as samples to conduct the conventional qPCR assay on PCR instrument and microfluidic LAMP assay on the customized chip and equipment. Table 2 illustrates the comparison of detection accuracy between qPCR and microfluidic LAMP among 48 positive samples and 48 negative samples. Based upon the above trails, we constructed ROCs to analyze the accuracy of the microfluidic detection system. The results in Fig. 6a demonstrate that the specificity and sensitivity of our microfluidic detection system were 91.7% and 100%, respectively. The microfluidic LAMP assay effectively discriminated HPV18-positive and -negative samples with an AUCroc of 0.958 ($p < 0.0001$) and a Youden index J of 0.9167, which supported the dependability of our diagnostic tool. Furthermore, the ROC curves of the qPCR assay and microfluidic LAMP assay were plotted and compared (Fig. 6b), which indicated no significant difference between these two methods with regard to HPV18 detection ($Z = 2.067$, $p = 0.0387$). The results manifested that the microfluidic detection system was comparable to conventional qPCR on account of its reasonable specificity and sensitivity.

Though qPCR assay is the gold standard, the characteristics such as time-consuming and repetitive cannot be ignored. Moreover, it is commonly known that nucleic acid extraction is tedious and complicated. Sophisticated procedures including solution dilution, distribution, precise temperature control and cycling are inevitable and require professionals and expensive instruments. Therefore, we compared the Tt values

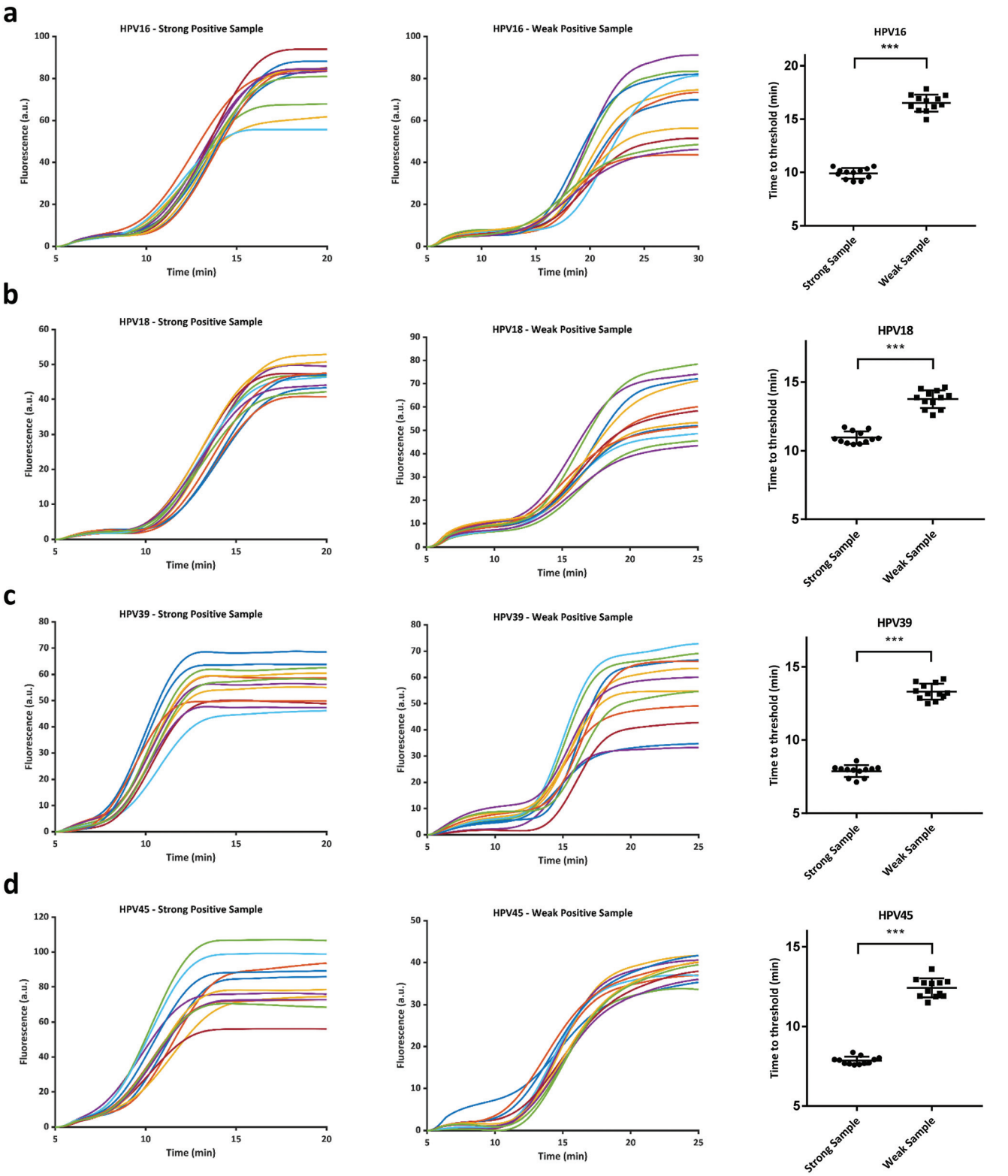

Fig. 5 Evaluation of the stability of the microfluidic detection system. The stability analysis and Tt values of (a) HPV16, (b) HPV18, (c) HPV39, (d) HPV45 and (e) HPV52. (f) SD and C.V. of Tt values for HPV16, HPV18, HPV39, HPV45 and HPV52. Each test item is certificated by twelve replicate trials with strong and weak positive samples, respectively. Replicate experiments are displayed in different colors for friendly observation. Data are presented as mean ± S.D., $*p < 0.05$, $**p < 0.01$, $***p < 0.001$.

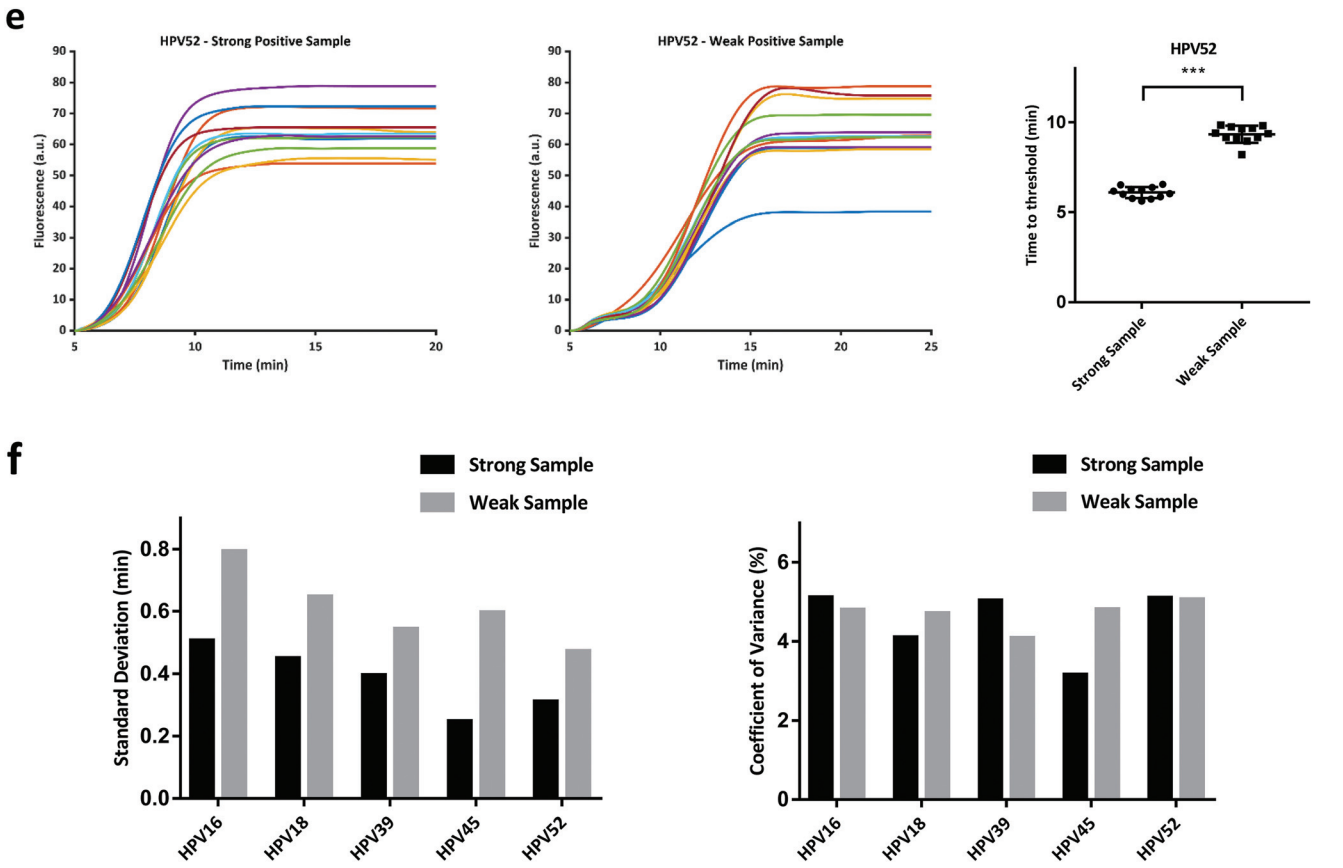

Fig. 5 *(Contd)*.

Table 2 Comparison of detection accuracy between qPCR and microfluidic LAMP

		qPCR		
		Positive	Negative	Total
Microfluidic LAMP	Positive	48	4	52
	Negative	0	44	44
Total		48	48	

between qPCR and microfluidic LAMP targeting HPV18, where we converted Ct values into Tt values in the qPCR according to standard cycling parameters (Fig. S3†). The results in Fig. 6c indicate the comparison of these two assays, and the average Tt values were 16.39 min and 10.56 min, respectively. Additionally, the exact Ct and Tt values of qPCR and LAMP assay are presented in Tables S6 and S7,† and the amplification curves of these two methods are displayed in Fig. S4 and S5.† The comparison of Tt values between qPCR and microfluidic LAMP indicated a substantial decline of amplification time in our methods. Simultaneously, when considering nucleic acid extraction and other transfer processes, it would take an extra 30 min to perform qPCR. At the same time, microfluidic LAMP detection only required 5 min to automatically complete the above-mentioned procedures because we integrated Chelex-100-based nucleic acid purification into the microfluidic chip and equipped it with the corresponding instruments. Thereby, our microfluidic detection system endeavoured to a more available nucleic acid diagnosis approach and exhibited irreplaceable advantages in shorter detection time and simple operation. At the same time, the detection accuracy is also acceptable regarding the qPCR assay as a solid standard. These results indicated the potential of our microfluidic detection system for rapid, effective and convenient diagnosis under the resource-limited circumstance, which offered an alternative choice for the conventional qPCR assay.

Future consideration

We proposed an integrated microfluidic detection system for automatic and rapid diagnosis of high-risk HPV with considerable performance in nucleic acid purification, isothermal amplification and fluorescence detection. This system is in full compliance with rapid diagnosis and provides an effective sample-in-answer-out analysis within 40 minutes, which is faster than the conventional qPCR assay or previous microfluidic detection devices.[26,39,49] It is able to conduct 40 LAMP reactions and detections simultaneously, in which the centrifugal platform promotes automated operation with minimal labour costs, fulfilling the purpose of high-throughput and large-scale preliminary nucleic acid detections. There is no sophisticated

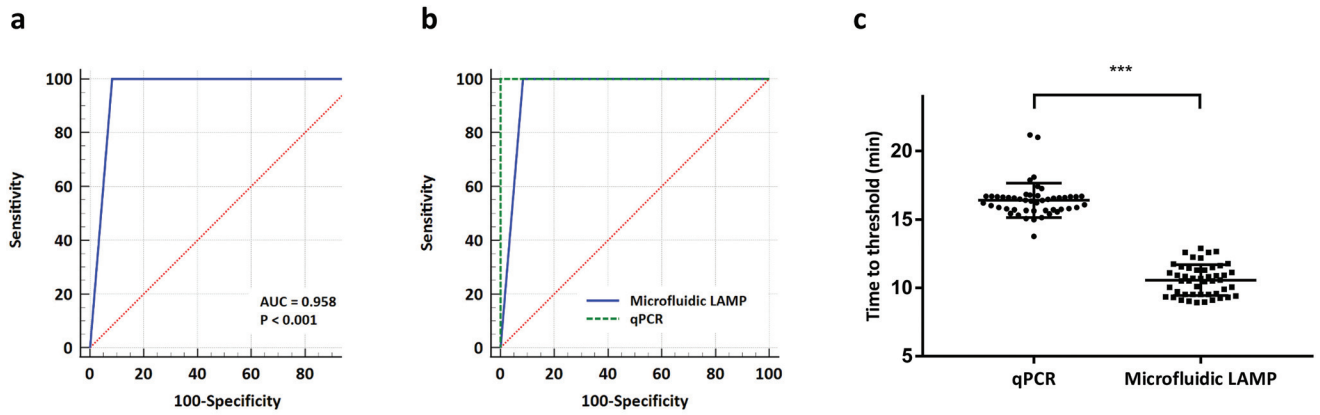

Fig. 6 Diagnostic performance of the microfluidic LAMP assay. (a) ROC analysis of the microfluidic detection system for HPV18 tests. (b) ROC analysis of the diagnostic performance of the microfluidic LAMP assay and qPCR assay. (c) Tt values of microfluidic LAMP assay and qPCR assay for HPV18 (n = 48). Data are presented as mean ± S.D., *p < 0.05, **p < 0.01, ***p < 0.001.

structure or complex DNA extraction method, significantly reducing the manufacturing costs of mass production. Moreover, the entire diagnostic process is completed without expensive instruments or professionals, even ordinary people with no medical training can handle it. To further save the reagents and cost, we also optimized the LAMP formula, reducing the final volume of individual reaction from the usual 25 μL to 8 μL. These improvements result in a shorter detection time, powerful diagnostic throughput and fewer reagents, which make this system particularly amenable for cost-effective POCT in poor settings. In the future, there are some opportunities to further extend the utility of the microfluidic detection system. For instance, this system is a universal platform for molecular diagnosis, which could be used in diverse biological detection rather than HPV tests only. To detect other pathogens, their corresponding freeze-dried primers are embedded into the reaction chambers, and the multiplexed diagnosis could be performed according to similar procedures as before. Taken together, the developed microfluidic detection system exhibits promising potential to be used in rural areas for large-scale preliminary selection. However, we acknowledge that our detection performance remains to be improved compared to digital LAMP,[39] which provides absolute quantitative results and excellent sensitivity and specificity. In future research, we will reconsider it and seek a balance between accessibility and accuracy. In addition, more clinical trials are demanded to confirm the practicality for broader application. Moreover, a user-friendly software needs to be developed for convenient generation and visualization of amplification curves, which facilitates precise quantitative analysis for non-professionals.

Conclusions

Efforts to improve diagnostic and prognostic tools could benefit from the accurate, accessible, affordable and all-in-one detection system, in which a microfluidic chip has crushed this field currently. In this study, we have successfully developed an automatic and rapid microfluidic detection system involving a microfluidic chip equipped with a centrifugal driver, a temperature controller and a fluorescence monitor, which integrated nucleic acid purification, isothermal amplification and real-time fluorescence detection. The centrifugal chip is simple, effective, requiring no sophisticated structure and easy to manufacturing. The proposed system integrates Chelex-100-based nucleic acid isolation and presents decent detection performance in terms of specificity of primer sets, stability, efficiency and accuracy for five high-risk HPV tests. The microfluidic LAMP assay is comparable to conventional qPCR assays, while our system requires fewer time costs and easy procedures. Briefly, owing to its high-throughput, simple-to-operate, sample-to-answer, cost-effective characteristics, *etc.*, which is reasonable, we believe that this microfluidic detection system could serve as a promising diagnostic tool in large-scale preliminary selection. Furthermore, this system holds broad application prospects in point-of-care nucleic acid detections, particularly in resource-limited situation.

Author contributions

Shengli Mi and Jiajun Huang conceived this study. Xiaoyu Zhao, Li Xiang and Jiajun Huang designed the experiments. Xiaoyu Zhao wrote and revised the manuscript. Xiaoyu Zhao, Li Xiang, Weihao Yang and Jiwei Peng performed the experiments, analyzed data and commented on the manuscript.

Conflicts of interest

The authors confirm that there are no conflicts to declare.

Acknowledgements

This work was funded by the Project of Basic Research of Shenzhen, China (JCYJ20180507183655307 & JCYJ20190813143221901).

Shengli Mi and Jiajun Huang received the funding. The funders had no role in study design, data collection and analysis, decision to publish, or preparation of the manuscript.

Notes and references

1 H. zur Hausen, *Nat. Rev. Cancer*, 2002, **2**, 342–350.
2 D. Maucort-Boulch, S. Franceschi, M. Plummer, L. Herrera, D. Loria, E. Matos, M. A. Prince, M. Molano, N. Muñoz, H. Posso, M. Ronderos, A. Arslan, G. Clifford, M. Dai, S. Vaccarella, J. Cherian, V. Ghisetti, A. Gillio-Tos, S. Gallus, G. Ronco, N. Segnan, H. R. Shin, D. H. Lee, I. Ajayi, K. Ojemakinde, A. Omigbodum, J. O. Thomas, A. Bardin, W. Zatonski, X. F. Bosch, R. Font, S. De Sanjose, A. Deechaisate, V. Kaenploy, V. Kesararat, S. Kongchuchuy, T. Kornsilp, S. Sukrivach, S. Tunsakul, P. Yingseri, C. J. L. M. Meijer, P. J. F. Snijders, M. Jacobs, P. T. H. Anh and N. T. Hieu, *Cancer Epidemiol. Biomarkers Prev.*, 2008, **17**, 717–720.
3 ICO, *Human Papillomavirus and Related Diseases Report*, 2016.
4 A. Gulliksen, H. Keegan, C. Martin, J. O'Leary, L. A. Solli, I. M. Falang, P. Grnn, A. Karlgrd, M. M. Mielnik, I. R. Johansen, T. R. Tofteberg, T. Baier, R. Gransee, K. Drese, T. Hansen-Hagge, L. Riegger, P. Koltay, R. Zengerle, F. Karlsen, D. Ausen and L. Furuberg, *J. Oncol.*, 2012, **2012**, DOI: 10.1155/2012/905024.
5 S. M. Kulmala, S. Syrjänen, I. Shabalova, N. Petrovichev, V. Kozachenko, J. Podistov, O. Ivanchenko, S. Zakharenko, R. Nerovjna, L. Kljukina, M. Branovskaja, V. Grunberga, A. Juschenko, P. Tosi, R. Santopietro and K. Syrjänen, *J. Clin. Microbiol.*, 2004, **42**, 2470–2475.
6 G. S. Ogilvie, D. Van Niekerk, M. Krajden, L. W. Smith, D. Cook, L. Gondara, K. Ceballos, D. Quinlan, M. Lee, R. E. Martin, L. Gentile, S. Peacock, G. C. E. Stuart, E. L. Franco and A. J. Coldman, *JAMA, J. Am. Med. Assoc.*, 2018, **320**, 43–52.
7 C. Ward, J. Pedraza, K. Kavanagh, I. Johannessen and K. Cuschieri, *J. Virol. Methods*, 2014, **207**, 128–132.
8 D. A. M. Heideman, A. T. Hesselink, J. Berkhof, F. Van Kemenade, W. J. G. Melchers, N. F. Daalmeijer, M. Verkuijten, C. J. L. M. Meijer and P. J. F. Snijders, *J. Clin. Microbiol.*, 2011, **49**, 3983–3985.
9 I. Hologic, *Aptima® HPV Assay*, 2015.
10 G. M. Whitesides, *Nature*, 2006, **442**, 368–373.
11 R. Gorkin, J. Park, J. Siegrist, M. Amasia, B. S. Lee, J. M. Park, J. Kim, H. Kim, M. Madou and Y. K. Cho, *Lab Chip*, 2010, **10**, 1758–1773.
12 M. Tang, G. Wang, S. K. Kong and H. P. Ho, *Micromachines*, 2016, **7**(2), DOI: 10.3390/mi7020026.
13 Y. Cheng, X. Zhang, Y. Cao, C. Tian, Y. Li, M. Wang, Y. Zhao and G. Zhao, *Appl. Mater. Today*, 2018, **13**, 116–125.
14 Y. Ren, L. M. C. Chow and W. W. F. Leung, *Biomed. Microdevices*, 2013, **15**, 321–337.
15 M. Geissler, D. Brassard, L. Clime, A. V. C. Pilar, L. Malic, J. Daoud, V. Barrère, C. Luebbert, B. W. Blais, N. Corneau and T. Veres, *Analyst*, 2020, **145**, 6831–6845.
16 Y. Zhao, Y. Hou, J. Ji, F. Khan, T. Thundat and D. J. Harrison, *Anal. Chem.*, 2019, **91**, 7570–7577.
17 A. Bruchet, V. Taniga, S. Descroix, L. Malaquin, F. Goutelard and C. Mariet, *Talanta*, 2013, **116**, 488–494.
18 S. T. Krauss, M. S. Woolf, K. C. Hadley, N. M. Collins, A. Q. Nauman and J. P. Landers, *Sens. Actuators, B*, 2019, **284**, 704–710.
19 W. Espulgar, W. Aoki, T. Ikeuchi, D. Mita, M. Saito, J. K. Lee and E. Tamiya, *Lab Chip*, 2015, **15**, 3572–3580.
20 L. Zhou, Y. Chen, X. Fang, Y. Liu, M. Du, X. Lu, Q. Li, Y. Sun, J. Ma and T. Lan, *Anal. Chim. Acta*, 2020, **1125**, 57–65.
21 G. Wang, J. Tan, M. Tang, C. Zhang, D. Zhang, W. Ji, J. Chen, H. P. Ho and X. Zhang, *Lab Chip*, 2018, **18**, 1197–1206.
22 H. Xiong, X. Ye, Y. Li, L. Wang, J. Zhang, X. Fang and J. Kong, *Anal. Chem.*, 2020, **92**, 14297–14302.
23 X. Ye, L. Li, J. Li, X. Wu, X. Fang and J. Kong, *ACS Sens.*, 2019, **4**, 3066–3071.
24 R. Wang, R. Zhao, Y. Li, W. Kong, X. Guo, Y. Yang, F. Wu, W. Liu, H. Song and R. Hao, *Lab Chip*, 2018, **18**, 3507–3515.
25 S. J. Oh, B. H. Park, G. Choi, J. H. Seo, J. H. Jung, J. S. Choi, D. H. Kim and T. S. Seo, *Lab Chip*, 2016, **16**, 1917–1926.
26 A. Sayad, F. Ibrahim, S. Mukim Uddin, J. Cho, M. Madou and K. L. Thong, *Biosens. Bioelectron.*, 2018, **100**, 96–104.
27 S. J. Oh and T. S. Seo, *Analyst*, 2019, **144**, 5766–5774.
28 J. H. Jung, B. H. Park, S. J. Oh, G. Choi and T. S. Seo, *Biosens. Bioelectron.*, 2015, **68**, 218–224.
29 H. Van Nguyen, V. D. Nguyen, E. Y. Lee and T. S. Seo, *Biosens. Bioelectron.*, 2019, **136**, 132–139.
30 D. Caetano-Anollés, *Polymerase Chain Reaction*, Elsevier Inc., 2013, vol. 5.
31 N. Tsugunori, O. Hiroto, M. Harumi, T. Yonekawa, W. Keiko, A. Nobuyuki and H. Tetsu, *Nucleic Acids Res.*, 2000, **28**, e63.
32 I. M. Lobato and C. K. O'Sullivan, *TrAC, Trends Anal. Chem.*, 2018, **98**, 19–35.
33 G. T. Walker, M. S. Fraiser, J. L. Schram, M. C. Little, J. G. Nadeau and D. P. Malinowski, *Nucleic Acids Res.*, 1992, **20**, 1691–1696.
34 H. Zhang, Y. Xu, Z. Fohlerova, H. Chang, C. Iliescu and P. Neuzil, *TrAC, Trends Anal. Chem.*, 2019, **113**, 44–53.
35 P. S. Walsh, D. A. Metzger and R. Higushi, *BioTechniques*, 2013, **54**, 134–139.
36 A. Glière and C. Delattre, *Sens. Actuators, A*, 2006, **130–131**, 601–608.
37 J. D. Smith, I. Chatzis and M. A. Ioannidis, *J. Can. Pet. Technol.*, 2005, **44**, 25–31.
38 D. Mark, S. Haeberle, T. Metz, S. Lutz, J. Ducrée, R. Zengerle and F. von Stetten, *International Conference on Micro Elec*, 2008, 611–614.
39 D. T. Chiu, J. Wang, J. P. Staheli, A. Wu, J. E. Kreutz, Q. Hu, J. Wang, T. Schneider, B. S. Fujimoto, Y. Qin, G. S. Yen, B. Weng, K. Shibley, H. Haynes, R. L. Winer and Q. Feng, *Anal. Chem.*, 2021, **93**, 3266–3272.

40 J. Yin, Y. Suo, Z. Zou, J. Sun, S. Zhang, B. Wang, Y. Xu, D. Darland, J. X. Zhao and Y. Mu, *Lab Chip*, 2019, **19**, 2769–2785.
41 S. M. Azimi, G. Nixon, J. Ahern and W. Balachandran, *Microfluid. Nanofluid.*, 2011, **11**, 157–165.
42 S. Wang, N. Liu, L. Zheng, G. Cai and J. Lin, *Lab Chip*, 2020, **20**, 2296–2305.
43 S. Y. Lim, T. J. Lee, S. Y. Shin, N. H. Bae, S. J. Lee and Y. M. Park, *Anal. Methods*, 2020, **12**, 1197–1202.
44 K. R. Jackson, J. C. Borba, M. Meija, D. L. Mills, D. M. Haverstick, K. E. Olson, R. Aranda, G. T. Garner, E. Carrilho and J. P. Landers, *Anal. Chim. Acta*, 2016, **937**, 1–10.
45 C. R. Reedy, J. M. Bienvenue, L. Coletta, B. C. Strachan, N. Bhatri, S. Greenspoon and J. P. Landers, *Forensic Sci. Int.: Genet.*, 2010, **4**, 206–212.
46 J. Park, D. H. Han, S. H. Hwang and J. K. Park, *Lab Chip*, 2020, **20**, 3346–3353.
47 P. Chen, C. Chen, Y. Liu, W. Du, X. Feng and B. F. Liu, *Sens. Actuators, B*, 2019, **283**, 472–477.
48 W. Gan, Y. Gu, J. Han, C. X. Li, J. Sun and P. Liu, *Anal. Chem.*, 2017, **89**, 3568–3575.
49 R. Tang, H. Yang, Y. Gong, M. L. You, Z. Liu, J. R. Choi, T. Wen, Z. Qu, Q. Mei and F. Xu, *Lab Chip*, 2017, **17**, 1270–1279.
50 K. Phillips, N. McCallum and L. Welch, *Forensic Sci. Int.: Genet.*, 2012, **6**, 282–285.
51 N. Simon, J. Shallat, C. Williams Wietzikoski and W. E. Harrington, *Biol. Methods Protoc.*, 2020, **5**, 1–7.
52 X. Ye, Y. Li, L. Wang, X. Fang and J. Kong, *Talanta*, 2021, **221**, 121462.
53 J. Carvalho, G. Puertas, J. Gaspar, S. Azinheiro, L. Diéguez, A. Garrido-Maestu, M. Vázquez, J. Barros-Velázquez, S. Cardoso and M. Prado, *Anal. Chim. Acta*, 2018, **1020**, 30–40.
54 Public Health England, *Understanding cycle threshold (Ct) in SARS-CoV-2 RT-PCR A guide for health protection teams*, 2020.
55 M. Shen, Y. Zhou, J. Ye, A. A. Abdullah AL-maskri, Y. Kang, S. Zeng and S. Cai, *J. Pharm. Anal.*, 2020, **10**, 97–101.
56 H. A. Erlich, D. Gelfand and J. J. Sninsky, *Science*, 1991, **252**, 1643–1651.
57 L. Schwarz, E. Freese, U. Gissmann, *et al.*, *Nature*, 1985, 111–114.